Will Perturbing Soil Moisture Improve Warm-Season Ensemble Forecasts? A Proof of Concept

Christian Sutton[1], Thomas M. Hamill[2], and Thomas T. Warner[3]

[1] *Program in Atmospheric and Oceanic Sciences*,
University of Colorado, Boulder, Colorado.
Current affiliation: Gulf Oil, Houston, Texas

[2] *NOAA-CIRES Climate Diagnostics Center, Boulder, Colorado*

[3] *Program in Atmospheric and Oceanic Sciences, University of Colorado*
and
National Center for Atmospheric Research, Boulder, Colorado

15 June 2005

Submitted to *Monthly Weather Review*

Corresponding author address:

Dr. Thomas M. Hamill
NOAA-CIRES Climate Diagnostics Center
Boulder, Colorado 80305-3328 USA
Phone: 1 (303) 497-3060
Fax: 1 (303) 497-6449
E-mail: tom.hamill@noaa.gov

ABSTRACT

Current generation short-range ensemble forecast members tend to be unduly similar to each other, especially for variables such as surface temperature. One possible cause of this is a lack of perturbations to the land-surface state. In this experiment, a two member-ensemble of the WRF model was run from two different soil moisture analyses. One-day forecasts were conducted for six warm-season cases over the central United States, both with explicitly resolved convection at 5-km grid spacing and with parameterized convection at 20-km grid spacing. At 5 km, the forecast differences due to changing the soil moisture were comparable to the differences in 20-km simulations with the same soil moisture but with a different convective parameterization. The differences of 20-km simulations from different soil moistures were less than the differences from changing the convective parameterization. Perturbing the state of the land surface is thus judged to be likely to improve operational short-range ensemble forecasts of precipitation and surface temperature, especially for explicitly resolved convective forecasts at high resolution.

1. **Introduction**

A goal of ensemble forecasting is to produce sharp, reliable probabilistic weather forecasts. Unfortunately, it is quite common for ensemble forecasts to be at least somewhat unreliable, i.e., tallying situations when 20 percent probability was forecast, the event did not happen 20 percent of the time. When ensemble forecasts are compared subsequently against observations, too often these observations will lie outside the span of the forecasts (Hamill and Colucci 1997). This problem is commonly worse for variables such as surface temperature or precipitation (e.g., Mullen and Buizza 2001, Fig. 15) than for midtropospheric variables (e.g., Buizza et al. 2000, Fig. 7).

Why is there an inadequate range of forecasts, and why does it affect surface variables more than other aspects of the model state? There are many possible explanations, such as inadequate resolution in ensemble members (Mullen and Buizza 2002, Szunyogh and Toth 2002, Buizza et al. 2003), suboptimal methods for generating initial conditions (Ehrendorfer and Tribbia 1997, Hamill et al. 2000, Hamill et al. 2003, Wang and Bishop 2003), and model biases related to problems in the parameterization of surface and boundary-layer effects and the diurnal cycle (e.g., Bright and Mullen 2002, Davis et al. 2003). While each of these may be very important, the one we choose to investigate here is the lack of perturbations to characteristics of the land-surface state. In most operational ensemble forecasts, the initial state of the atmosphere differs among ensemble members, but the initial state of the land surface is the same. If indeed the subsequent weather forecast is sensitive to perturbations to the land-surface state within the range of their uncertainty, then it may prove beneficial to perturb them in ensemble forecasts (Hamill 1997, Hamill and Colucci 1998).

In meteorological situations where ample solar radiation (insolation) reaches the ground, errors in the state of the land surface may affect the subsequent weather forecast. As the ground surface heats up during the day, sensible energy is transferred to the atmosphere, moisture evaporates from the soil or transpirates from plants (latent heating), and the soil below is heated. The partitioning of the available energy among sensible, latent, and ground heat fluxes depends on many variables, in particular soil moisture. Generally, the drier the soil, the smaller the daytime latent-heat flux, the larger the sensible-heat flux, the greater the warming of the air above, and the deeper the boundary layer (Philip 1957, Sasamori 1970, Pielke 2001). The partitioning also may be sensitive to a change in the roughness lengths (Zhang and Anthes 1982, Diak 1986) or other aspects such as soil textural characteristics (Ek and Cuenca 1994) or mis-specification of vegetation characteristics (Sellers et al. 1986, Xue et al. 1991).

There is a large body of literature demonstrating that mesoscale atmospheric circulations can be driven by regional differences in the land-surface state, circulations that in certain circumstances can determine where penetrative convection will develop (Ookouchi et al. 1984, Diak et al. 1986, Benjamin and Carlson 1986, Lanicci et al. 1987, Lakhtakia and Warner 1987, Yan and Anthes 1988, Chang and Wetzel 1991, Fast and McCorcle 1991, Betts et al. 1996, Chen et al. 2001). By extension, then, it is reasonable to hypothesize that an error in the land-surface state may change some of the details of the forecasts of penetrative convection, adding spread in warm-season ensemble forecasts of precipitation and near-surface variables.

The question we thus consider is whether realistic differences in the initial land-surface state will be large enough to substantially alter the location, timing, and intensity

of convection in high-resolution, short-term numerical weather forecasts. If one member contains a best guess at the land-surface state and another member contains a realistic perturbed guess, will the two members produce substantially different forecasts? A synoptic evaluation of a dryline case (Trier et al. 2004) showed that changing from a coarse-resolution, less sophisticated soil moisture analysis to a fine-resolution, more sophisticated one increased the realism of the forecast convection. The timing and location of the convection was substantially different between the two simulations. Sensitivity to soil moisture was also demonstrated in Hamill and Colucci (1998) and Gallus and Segal (2000). Crook (1996) similarly demonstrated that minor changes to the low-level thermodynamic structure (of the sort we hypothesize could be introduced by changing the soil moisture) could dramatically alter convective forecasts.

The article will provide a proof of concept of the sensitivity of selected summertime weather forecasts to modest changes in the soil moisture state. Provided with two soil moisture analyses that define different but equally valid estimates, will the subsequent weather forecasts differ? We examine short-range forecasts from six cases, two cases discussed in depth in this article and the remaining four in an online appendix. We will use the Weather-Research and Forecast (WRF) model at convection-resolving resolution (~5 km) and with parameterized convection (~20 km), and we compare the resulting differences in 2-m temperature and accumulated rainfall forecasts initialized with identical atmospheric conditions but different soil moistures. For the 20-km forecasts, we will compare the differences stimulated by the different soil moistures to differences resulting from using distinct cumulus convection schemes, which previously

has been shown to introduce sizeable differences in warm-season ensemble forecasts (Stensrud et al. 2000, Stensrud and Weiss 2002, Gallus 1999).

This article will not provide an operational technique for generating 10 or 100 realistic soil moisture perturbations. This will be left for future research; our intent is to demonstrate that perturbing the soil moisture in operational short-range ensemble forecasts is likely to have beneficial effects on probabilistic precipitation and surface-temperature forecasts by increasing the spread. We also have chosen to demonstrate the sensitivity only in the first 24 h. The mechanisms for upscale propagation of errors beyond 24 h are by now well known (e.g., Tribbia and Baumhefner 2004 and references therein).

Section 2 will describe the WRF model setup and the soil moisture analyses. Section 3 will provide detailed results for two of the six cases; the remaining four are described in the online appendix. Section 4 provides conclusions.

2. **Experimental design**

a. WRF model configuration.

WRF is a non-hydrostatic, Eulerian mesoscale model (Klemp et al. 2000, Michalakes et al. 2001, Skamarock et al. 2001, Wicker and Skamarock 2002). Two sets of simulations were run, each in two configurations. The first set utilized a ~20 km grid spacing and 31 vertical levels with parameterized convection and a domain (the outer rectangle in Fig. 1) approximately encompassing the conterminous United States (US).

The simulations in the second set were nested, with the inner domain run at ~ 5km and 31 levels, with explicitly resolved convection. The location of the inner domains (Fig. 1) changed depending on the case. The following approaches were used to represent physical processes: cloud microphysics were parameterized according to Lin (1983), longwave radiation parameterization was represented through the "RRTM" of Mlawer et al. (1997), shortwave radiation was based on Dudhia (1989), and the Mellor-Yamada-Janjic approach was used for the boundary-layer parameterization (Janjic 1996, 2002). The NOAH land-surface model was used (Chen and Dudhia 2001) as well as the data sets of land-surface characteristics accompanying this model. For most experiments, the 20-km simulations used the Kain-Fritsch (KF) convective parameterization (Kain and Fritsch 1990 , 1993). For comparison, some 20-km simulations also were performed with the Betts-Miller-Janjic (BMJ) convective parameterization (Betts and Miller 1986, Janjic 1994). The specific set of experiments that were performed will be described in Section 2c below.

b. Initial and boundary conditions.

The analyzed atmospheric and lateral boundary conditions were produced by the Eta Data Assimilation System, or "EDAS;" documentation is available at http://www.emc.ncep.noaa.gov/mmb/gcip.html . The data were archived on a Lambert-conformal grid with a nominal grid spacing of ~ 40 km. The modeling system was described in Rogers et al. (1995, 1996) and the archive is at the National Center for Atmospheric Research (dataset 609.2).

Two initial soil moisture states were used, both produced under the North American Land-Data Assimilation Scheme (LDAS) project described in Mitchell et al. (2004). Identical observed meteorological forcings (temperature, humidity, wind speed, observed precipitation) and land-surface characteristics were used as inputs to the stand-alone NOAH land-surface model (LSM; Chen and Dudhia 2001) and the MOSAIC LSM (Koster and Suarez 1996). One of the outputs of each LSM was a diagnosed profile of soil moisture. While the atmospheric forcings were the same for both models, the internal model physics were different enough so that over a long period of time, the soil moisture estimates grew increasingly different, each varying about their own climatological mean (Mahanama and Koster 2003). Interestingly, in these LSMs, the soil moisture is not considered to be a quantity that is important to analyze correctly in and of itself; what is important is that each LSM should provide reasonable accurate estimates of heat and moisture fluxes as part of their own modeling system, and each LSM achieves similarly reasonable fluxes from different soil moistures (Koster and Milly 1997).

For our purposes, this may indicate that a MOSAIC analyzed soil moisture state could potentially produce unrealistic forecast fluxes when used to initialize a forecast model with a NOAH LSM, as in our WRF experiments. In the simulations presented hereafter, the differences in midday, clear-sky sensible heat fluxes due to a change in soil moisture were typically 70 – 100 Wm^{-2}, a relatively large value. Results from Chen et al. (1996) compared differences between flux measurements and modeled fluxes using an earlier version of NOAH. There were several days when the flux differences were greater than 50 Wm^{-2}, even in a controlled setting where inputs to the LSM could be more carefully specified than in real-world NWP forecasts; hence 70 – 100 Wm^{-2} is not

necessarily unrealistic. Also, the differences in our two chosen soil moisture estimates were meant to initiate differences in surface fluxes that could be attributable to any component of the land-surface state that may have been improperly estimated. As previously mentioned, errors in the roughness length, soil texture, vegetation characteristics, and so on can induce errors in forecast surface fluxes. We have chosen the simpler approach of perturbing one variable by a larger amount rather than many variables by somewhat smaller amounts. As will be shown later, however, the WRF is capable of responding very non-linearly, producing forecast differences even from much smaller perturbations.

c. *Simulations performed*.

The set of five model simulations performed on each day are shown in Table 1. Each case day involves a summertime simulation under weak or moderate flow, and in each there was an area of intense rainfall stimulated by surface-based convection. The cases were also selected to have soil moistures in the moderate range. These five simulations include nested simulations from the two different soil moisture states, with outer and inner grid spacings of 20 and 5 km. The outer grid, encompassing the conterminous US (Fig. 1) used the Kain-Fritsch (KF) convective parameterization, while the inner grid used explicit convection. Since we focus on convection in the 5-km nested region, these two simulations are called "NOAH5" and "MOSAIC5," the name reflecting which soil moisture analysis was used. Additionally, the simulations were run at 20 km excluding the inner domain, and these simulations were names "NOAH20KF" and

"MOSAIC20KF." A final simulation was done at 20 km using the NOAH analysis and the Betts-Miller-Janjic (BMJ) convection scheme, "NOAH20BMJ." The reason for performing the simulations at 5 and 20 km were to determine if the sensitivity to soil moisture was qualitatively different with higher resolution and explicitly resolved convection. The test at 20 km with the BMJ permits a comparison of sensitivity to soil moisture and sensitivity to the convective parameterization (Gallus 1999, Stensrud et al. 2000, Stensrud and Weiss 2002).

Six different case days were examined, and on each day the forecasts were initialized at 1200 UTC and run for 24 h. All of the cases selected were summertime cases. We hypothesize that the changes to weather forecasts due to a change in surface fluxes should be more evident when insolation is large. We also chose to examine cases where the synoptic forcing was not particularly strong; again, one would not expect the soil moisture errors to stimulate much forecast error if an area is already covered by dense cloud and rain. The chosen days were 12 July 2001, 22 August 2001, 11 June 2002, 24 July 2002, 27 July 2002, and 11 August 2002. The article will examine 12 July 2001 and 24 July 2002; the remaining cases are described in the online appendix.

3. **Results**.

a. 12 July 2001

Figure 2a shows the sea-level pressure and the 500 hPa geopotential height used to initialize this model run. A broad ridge at 500 hPa was evident with its axis along the

Rockies, with relatively weak flow through most of the center of the country. A surface-pressure trough extended from the low-pressure system east of Maine, along the Atlantic seaboard, and then back through central Mississippi, Oklahoma, and into eastern Montana. The 24-h analyzed precipitation in Fig. 2b (taken from the ~32 km North American Regional Reanalysis, Mesinger et al. 2005) shows an extensive area of rainfall from southern Missouri south to the Gulf Coast, with more precipitation in western Kansas and eastern Colorado. For this experiment, we located the fine-mesh domain to cover the precipitation feature in the Mississippi River Valley (Fig. 1), where there was a maximum of greater than 40 mm of rainfall in central Arkansas and western Mississippi, as well as scattered reports of small hail and damaging winds. The NOAH soil moisture analysis (Fig. 2c) in this region showed generally moderate soil moisture amounts, though moister areas were found in western Missouri and southern Louisiana. Relative to NOAH, the top-layer MOSAIC soil moisture was more commonly drier (Fig 2d).

Consider the NOAH5 simulated rainfall in Fig, 2e, accumulated over 24 h. The pattern of heavy rainfall was in a similar region to where heavy rain was observed, though the forecast maximum in central Arkansas was slightly east of where it was observed. Figure 2f shows the difference in accumulated precipitation between the MOSAIC5 and NOAH5 simulations. The precipitation differences were often quite large in magnitude, often 20 cm or more. The general region where the precipitation occurred was similar, but the exact location of the convective cells often differed by ~50 km. In some situations, this may have led to a somewhat better forecast. For example, the MOSAIC5 simulation was somewhat moister further west in Arkansas and produced more precipitation in central and southern Mississippi, as was observed. Considering the

12-h 2-m temperature forecasts at 0000 UTC 13 July 2001 (Fig. 2g), a strong temperature contrast was evident in central Arkansas, delineating the boundary at that time between the convectively modified air to the north (Fig. 3j) and the pre-convective environment to the south. Figure 2h shows that in some areas there were as much as 5 C differences between the simulated 2-m temperatures in the MOSAIC5 and NOAH5 runs. Most notably, due to differences in the intensity of convection over Louisiana and Mississippi (Fig. 3k), there were relatively large differences in the 2-m temperature forecasts, with the areas affected by convectively initiated cold pools differing between the simulations.

Figure 3 shows the 3-hourly accumulations in the NOAH5 simulation as well as the differences between MOSAIC5 and NOAH5. An additional set of simulations was also conducted, whereby the differences in soil moisture were scaled down to 10 percent of their original size, i.e., the MOSAIC5 soil moisture was replaced by the NOAH5 soil moisture plus 10 percent of the difference between MOSAIC5 and NOAH5, and the precipitation differences are shown for this case as well. Interestingly, the differences were nearly as large for the simulation with the 90 percent smaller soil moisture perturbation. Even with the smaller perturbation, convection triggered in slightly different locations. Thus the response to initial perturbations can be strongly non-linear in the presence of convection. As soon as convection initiated at different grid points in the two simulations, regardless of whether this happened as a consequence of a small or large soil moisture perturbation, the pair of precipitation forecasts quickly became very different. This may exemplify the rapid error growth up from the small scales posited by Lorenz (1969).

The simulations were also performed at 20 km grid spacing using the Kain-Fritsch convective parameterization (NOAH20KF and MOSAIC20KF). Figure 4 provides the precipitation and temperature forecast information for these simulations. Figure 4a shows that the NOAH20KF precipitation in Arkansas was located ~100-150 km to the east of the band from the NOAH5 simulation in Fig. 2e. The highest precipitation totals from MOSAIC20KF were displaced to the west of the band in the NOAH20KF (Fig. 4b). Outside of the region around Memphis, Tennessee, where the two simulations were very different, the precipitation differences were typically smaller than the differences at 5 km with explicit convection. The temperature differences were smaller, too (Fig. 4c-d) , and didn't produce large areas of differences caused by changing cold pool locations.

Consider the general sensitivity to the soil moisture compared to the sensitivity due to choice of convective parameterization. Figure 5a shows the precipitation from the NOAH20KF and NOAH20BMJ simulations. The differences in precipitation amount and 2-m temperature forecasts are shown in Figures 5 b-c. The differences in precipitation were comparable in magnitude to the differences between the NOAH5 and MOSAIC5 simulations (Fig. 2f), but here the differences tended to be much larger in scale; the NOAH20BMJ produced much less widespread convection over the Gulf Coast and up the Atlantic seaboard than the NOAH20KF. Temperature differences of 1-2 K or larger were quite widespread, related to differences in the areas where convection was forecast and the subsequent parameterization of moist downdrafts in the two schemes (see also Wang and Seaman 1997).

This case demonstrates that sizeable differences in precipitation and surface temperatures can be induced by differences in the soil moisture. The soil moisture did

not radically change the area where convection occurred, but differences at individual grid points were often very large, due to small displacements of the convective elements.

b. 24 July 2002

For this case, at 1200 UTC, a weak surface ridge extended from Wyoming to western Texas (Fig. 6a), and a trough of low pressure extended southeast from eastern Montana, with a region of strong southerly flow over the eastern Dakotas. Zonal flow predominated at 500 hPa over the northern tier of states. Precipitation was observed in the northern Great Plains states, along the Texas border with Oklahoma and Louisiana, along the Florida Gulf Coast, and up through the Carolinas (Fig. 6b). Several tornadoes occurred in central Nebraska on this day, and there were widespread reports of hail and damaging wind in Nebraska and the Dakotas. We located our 5-km domain to cover the precipitation maximum in the northern Great Plains states (Fig. 1). The top-layer NOAH analyzed soil moisture (Fig. 6c) shows modestly moist soils east of central Iowa, with drier soils to the west. The top-layer MOSAIC soil moisture was even drier across much of the Great Plains (Fig. 6d), with a small patch of wetter soil occurring over west central Illinois. However, over many parts of Nebraska, the subsoil layers were moister in MOSAIC than in NOAH (not shown).

The NOAH5 simulation produced a band of intense precipitation (Fig. 6e) over the border of Iowa and Minnesota. The highest accumulated forecast totals were in excess of 80 mm. The precipitation maximum was forecast to the east of where it was actually observed (Fig. 6b) and forecast more than observed. Comparing the difference between the MOSAIC5 and NOAH5 simulations (Fig. 6f), the MOSAIC5 simulation

produced a more intense band to the northeast of the band in NOAH5, a more intense second band through central-northern Minnesota, and a more intense third band in northwest Iowa, closer to the observed maxima. Compared to the previous 12 July 2001 case, the precipitation differences were larger in scale.

The NOAH5 simulation produced a strong 2-m temperature gradient at 12 h in northeast Nebraska, dividing the convectively modified and pre-convective air masses. The MOSAIC5 simulation was slightly warmer (Fig. 6h) over southwest Minnesota and in a NW-SE band from SE South Dakota to NW Iowa, reflecting a slightly delayed southwesterly propagation of the cold pool in the MOSAIC5 simulation. Elsewhere, it was as much as 2-5 C cooler than the NOAH forecast over a wide area in eastern Kansas, Nebraska, South Dakota, and North Dakota. The lower temperatures in the MOSAIC5 were attributable to less sensible and more latent heating as a result of the higher sub-surface soil moistures in MOSAIC.

Figure 7a shows the forecast 24-h precipitation totals for the NOAH20KF simulation. The highest forecast accumulations were 40 - 60 mm, heavier than observed (Fig. 6b) but somewhat lighter than the 5-km forecast (Fig. 6e) and closer to the position of the observed maximum. Figure 7b shows that the maximum from the MOSAIC20KF forecast occurred to the east of the maximum in NOAH20KF, with generally lighter amounts elsewhere. The differences again were relatively larger in scale than in the 12 July 2001 case. The 2-m temperature forecast in Fig. 7c was similar to that from the NOAH5 (Fig. 6g). Temperature differences of 1 C or larger were common, even in areas outside of the region of convection.

The precipitation forecast differences (Fig. 8b) resulting from the use of the BMJ

parameterization (Fig. 8a) were rather similar to the differences introduced by varying the soil moisture, though somewhat lesser in magnitude in this case. Surface-temperature differences (Fig. 8c) were also a bit smaller than those introduced by varying the soil moisture.

The remaining four cases are described in the online appendix.

c. Synthesis of statistics from all cases

Figure 9 presents the statistics on how much variability was introduced to 24-h precipitation and 12-h surface-temperature forecasts by varying the soil moisture or the convective parameterization. We consider the MOSAIC5-NOAH5, MOSAIC20KF-NOAH20KF, and the NOAH20BMJ-NOAH20KF differences, stratified by the grid-point precipitation amount of the control forecasts in each case (NOAH5, NOAH20KF, and NOAH20KF, respectively). In the case of MOSAIC5-NOAH5, the gridded forecasts were averaged to 20 km, so the statistics were done on a comparable grid; on the figure, these data are labeled "$<\text{MOSAIC5-NOAH5}>_{20}$". All data are presented only over the region of the inner domain.

From Fig. 9, we see that when little or no rain was forecast in the control, typically changing the soil moisture did not change this. When heavy rain was forecast, then relatively large changes commonly occurred as a result of changing soil moisture or convective parameterization. The changes at 5 km due to changing the soil moisture were comparable to the changes at 20 km due to varying the convective parameterization. The precipitation changes at 20 km due to changing the soil moisture were smaller than at 5 km, though from the individual maps, the reader can see that the effects were often

large in several of the cases. For surface temperature forecasts (Fig. 9b), approximately 10 percent of the grid points had their 12-h forecast of surface temperature changed by 1 K or more in each sensitivity study, indicating that the soil moisture can be a source of short-range surface temperature forecast variability in some regions.

Examining the frequency at which the precipitation amount forecasts were issued (Fig. 10), the BMJ parameterization produced heavy precipitation less frequently than the KF. The explicit convection forecasts at 5 km produced less light and more heavy precipitation events than the 20-km parameterized convection. Changing the soil moisture initial condition did not change the precipitation frequency distribution very much (not shown); the apparent "bias" in Fig. 9a of $<\text{MOSAIC5-NOAH5}>_{20}$ at high precipitation amounts is illusory. What this diagram indicates is that in situations where NOAH5 forecast very heavy precipitation, typically MOSAIC5 forecast less. However, there were many cases when NOAH5 forecast lesser amounts and much heavier rain was forecast in MOSAIC5 (hence the outlying dots are skewed toward heavier MOSAIC5 precipitation amounts).

Overall, these results confirm the impression presented by studying the weather maps that perturbing the soil moisture did not tend to alter the general region where convection was forecast, but it introduced variability in the amount, with more variability introduced in regions where the control forecast large amounts. The result of not altering the region where convection was forecast is somewhat different than a result presented in a preliminary sensitivity study (Hamill and Colucci 1998, Fig. 3 a-b). In one case study there, an intense band of precipitation was forecast from one soil moisture, while nearly none was forecast from a slightly different soil moisture. Perhaps if we had examined

more than the six cases presented here, we would have seen similar examples of radically different precipitation forecasts, where convection was triggered in one simulation but not another.

4. **Conclusions**.

In this study, we examined short-range warm-season temperature and precipitation forecast sensitivity due to changing the source of the soil moisture analysis. Our hypothesis was that in some situations, a modest change in the soil moisture could substantially change the short-range weather forecast by altering the timing and location of convective precipitation. If this was the case, then perturbing the soil moistures may add some spread to short-range ensemble weather forecasts, which typically have member forecasts that are unduly similar.

The results presented here show that short-term temperature and precipitation forecasts can indeed be changed as a consequence of changing the soil moisture. The changes to 5-km forecasts due to soil moisture differences were almost as large as the changes to 20-km forecasts due to using an alternate convective parameterization, previously determined to be a large source of uncertainty in ensemble forecasts. Changing the soil moisture of 20-km forecasts introduced less variability on average, but for several of the case days, the differences between the simulations were quite large.

We expect then that perturbing soil moisture initial conditions ought to have a beneficial impact on the skill of short-range probabilistic forecasts of surface temperature and precipitation during the warm season. While this study did not address how to

generate a large ensemble of these differences, generating a perturbation methodology is hardly an insurmountable problem. Perhaps perturbations could be generated by randomly sampling from a time series of differences between soil moisture analyses from different sources, or perhaps the initial conditions from an ensemble Kalman filter of soil moisture analyses could be used (e.g., Reichle et al. 2002 ab).

Acknowledgments

NSF grant ATM-0130154 fully supported the graduate education of the lead author and supported the other authors for their involvement in this project. We thank Fei Chen and Jason Knievel (NCAR), Jeff Weiss (University of Colorado), and Georg Grell (NOAA/FSL) for their consultation on this project.

References

Benjamin, S. G., and T. N. Carlson, 1986: Some effects of surface heating and topography on the regional storm environment. Part 1: three-dimensional simulations. *Mon. Wea. Rev.*, **114**, 307-329.

Betts, A. K., M. J. Miller, 1986: A new convective adjustment scheme. Part II: Single column test using GATE wave. BOMEX, ATEX and Arctic airmass data sets. *Quart. J. Royal Meteor. Soc*., **112**, 693-709.

Betts, A. K., J. H. Ball, A. C. Beljaars, M. J. Miller, and P. A. Viterbo, 1996: The land surface-atmosphere interaction: a review based on observational and global modeling perspectives. *J. Geophys. Res*., **101D**, 7209-7225.

Bright, D. R., and S. L. Mullen, 2002: Short-range ensemble forecasts of precipitation during the southwest monsoon. *Wea. Forecasting*, **17**, 1080-1100.

Buizza, R., J. Barkmeijer, T. N. Palmer, and D. S. Richardson, 2000: Current status and future developments of the ECMWF ensemble prediction system. *Meteor. Appl.*, **7**, 163-175.

---------- , D. S. Richardson, and T. N. Palmer, 2003: Benefits of increased resolution in the ECMWF ensemble prediction system and comparison with poor man's ensembles. *Quart. J. Royal Meteor. Soc.*, **129**, 1269-1288.

Chang, J.-T., and P. J. Wetzel., 1991: Effects of spatial variations of soil moisture and vegetation on the evolution of a pre-storm environment: a numerical case study. *Mon. Wea. Rev*., **119**, 1368-1390.

Chen, F., K. E. Mitchell, J. Schaake, Y. Xue, H.-L. Pan, V. Koren, Q. Y. Duan, M. Ek, and A. K. Betts, 1996: Modeling of land-surface evaporation by four schemes and comparison with FIFE observations. *J. Geophys. Res*., **101D**, 7251-7268.

---------- , T. T. Warner, and K. Manning, 2001: Sensitivity of orographic moist convection to landscape variability: a study of the Buffalo Creek, Colorado, flash flood case of 1996. *J. Atmos. Sci*., **58**, 3204-3223.

---------- , and J. Dudhia, 2001: Coupling an advanced land-surface/hydrology model with the Penn State/NCAR MM5 modeling system. Part I: model implementation and sensitivity. *Mon. Wea. Rev*., **129**, 569-585.

Crook, N. A., 1996: Sensitivity of moist convection forced by boundary-layer processes to low-level thermodynamic fields. *Mon. Wea. Rev*., **124**, 1767-1785.

Davis, C. A., K. W. Manning, R. E. Carbone, S. B. Trier, and J. D. Tuttle, 2003: Coherence of warm-season continental rainfall in numerical weather prediction models. *Mon. Wea. Rev*., **131**, 2667-2679.

Diak, G., S. Heikkinen, and J. Bates, 1986: The influence of variations in surface treatment on 24-hour forecasts with a limited area model, including a comparison of modeled and satellite-measured surface temperatures. *Mon. Wea. Rev*., **114**, 215-232.

Dudhia, J., 1989: Numerical study of convection observed during the winter monsoon experiment using a mesoscale two-dimensional model. *J. Atmos. Sci*., **46**, 3077-3107.

Ehrendorfer, M., and J. J. Tribbia, 1997: Optimal prediction of forecast error covariances through singular vectors. *J. Atmos. Sci*., **54**, 286-313.

Ek, M., and R. H. Cuenca, 1994: Modeling surface fluxes and boundary layer development. *Boundary Layer Meteor.*, **70**, 369-383.

Fast, J. D., and M. D. McCorcle, 1991: The effect of heterogeneous soil moisture on a summer baroclinic circulation in the central United States. *Mon. Wea. Rev.*, **119**, 2140-2167.

Gallus, W. A., 1999: Eta simulations of three extreme precipitation events: sensitivity to resolution and convective parameterization. *Wea. Forecasting*, **14**, 405-426.

---------- , and M. Segal, 2000: Sensitivity of forecast rainfall in a Texas convective system to soil moisture and convective parameterization. *Wea. Forecasting*, **15**, 509-525.

Hamill, T. M., and S. J. Colucci, 1997: Verification of Eta-RSM short-range ensemble forecasts. *Mon. Wea. Rev.*, **125**, 1312-1327.

----------, 1997: *Short-range ensemble forecasting using the Eta/RSM forecast models*. Ph. D. dissertation, Cornell University, Ithaca, NY. Available from UMI Dissertation Services, 300 N. Zeeb Rd., P. O. Box 1346, Ann Arbor, MI 48106-1346.

----------, and ----------, 1998: Perturbations to the land surface condition in short-range ensemble forecasts. *Preprints, 12hth Conf. Numerical Weather Prediction* [Phoenix, AZ]. American Meteorological Society, 273-276.

----------, C. Snyder, and R. E. Morss, 2000: A comparison of probabilistic forecasts from bred, singular vector, and perturbed observation ensembles. *Mon. Wea. Rev.*, **128**, 1835-1851.

----------, ----------, and J. S. Whitaker, 2003: Ensemble forecasts and the properties of flow-dependent analysis-error covariance singular vectors. *Mon. Wea. Rev.*, **131**, 1741-1758.

Janjic, Z. I., 1994: The step-mountain Eta coordinate model: further developments of the convection, viscous sublayer, and turbulence closure schemes. *Mon. Wea. Rev.*, **122**, 927-945.

---------- , 1996: The surface layer in the NCEP Eta Model. Preprints, *11th Conf. on Numerical Weather Prediction* [Norfolk, VA]. American Meteorological Society, 354-355.

---------- , 2002: Nonsingular implementation of the Mellor-Yamada level 2.5 scheme in the NCEP Meso model. *NCEP Office Note No. 437*, 61 pp.

Kain, J. S., and J. M. Fritsch, 1990: A one-dimensional entraining/ detraining plume model and its application in convective parameterization. *J. Atmos. Sci.*, **47**, 2784-2802.

----------, and ----------, 1993: Convective parameterization for mesoscale models: The Kain-Fritsch scheme. In *The Representation Of Cumulus Convection Indiana Numerical Models*, K. A. Emanuel and D.J. Raymond, Eds., Amer. Meteor. Soc., 246 pp.

Klemp, J. B., W. C. Skamarock, and J. Dudhia, 2000: Conservative split-explicit time integration methods for the compressible nonhydrostatic equations. Available at http://www.mmm.ucar.edu/wrf/users/pub-doc.html.

Koster, R. D., and M. J. Suarez, 1996: Energy and water balance calculations in the Mosaic LSM, *NASA Tech. Memo*. 104606, vol. 9, 58 pp.

Koster, R. D., and P. C. D. Milly, 1997: The interplay between transpiration and runoff formulations in land surface schemes used with atmospheric models. *J. Climate*, **10**, 1578-1591.

----------, and M. J. Suarez, 1996: Energy and water balance calculations in the Mosiac LSM. *NASA Tech. Memo 104606*, Vol. 9, 60 pp.

Lakhtakia, M. N., and T. T. Warner, 1987: A real-data numerical study of the development of precipitation along the edge of an elevated mixed layer. *Mon. Wea. Rev.*, **115**, 156-168.

Lanicci, J. M., T. N. Carlson, and T. T. Warner, 1987: Sensitivity of the Great Plains severe storm environment to soil moisture distribution. *Mon. Wea. Rev.*, **115**, 2660-2673.

Lin, Y.-L., R. D. Farley, and H. D. Orville, 1983: Bulk parameterization of the snow field in a cloud model. *J. Climate Appl. Meteor*., **22**, 1065-1092.

Lorenz, E. N., 1969: The predictability of a flow which possesses many scales of motion. *Tellus*, **21**, 289-307.

Mahanama, S. P. P., and R. D. Koster, 2003: Intercomparison of soil moisture memory in two land surface models. *J. Hydrometeor*., **4**, 1134-1146.

Mesinger, F., G. DiMego, E. Kalnay, P. Shafran, W. Ebisuzaki, D. Jovic, J. Woollen, K. Mitchell, E. Rogers, M. Ek, Y. Fan, R. Grumbine, W. Higgins, H. Li, Y. Lin, G. Manikin, D. Parrish, and W. Shi, 2005: North American Regional Reanalysis. *Bull. Amer. Meteor. Soc*., submitted.

Michalakes, J., S. Chen, J. Dudhia, L. Hart, J. Klemp, J. Middlecoff, and W. Skamarock, 2001: Development of a next generation regional weather research and forecast

model. *Developments in Teracomputing: Proceedings of the Ninth ECMWF Workshop on the Use of High Performance Computing in Meteorology*, W. Zwieflhofer and N. Kreitz, Eds., World Scientific, 269–276.

Mitchell, K. E., and others, 2004: The multi-institution North American land data assimilation system (NLDAS): utilizing multiple GCIP products and partners in a continental distributed hydrological modeling system. *J. Geophys. Res*., **107D**, D07S90.

Mlawer, E. J., S. J. Taubman, P. D. Brown, M. J. Iacono, and S. A. Clough, 1997: Radiative transfer for inhomogeneous atmosphere: RRTM, a validated correlated-k model for the long-wave. *J. Geophys. Res*., **102D** , 16663-16682.

Mullen, S. L., and R. Buizza, 2001: Quantitative precipitation forecasts over the United States by the ECMWF ensemble prediction system. *Mon. Wea. Rev*., **129**, 638-663.

----------, and ----------, 2002: The impact of horizontal resolution and ensemble size on probabilistic forecasts of precipitation by the ECMWF ensemble prediction system. *Wea. Forecasting*, **17**, 173-191.

Ookouchi, Y., M. Segal, R. C. Kessler, and R. A. Pielke, 1984: Evaluation of soil moisture effects on the generation and modification of mesoscale circulations. *Mon. Wea. Rev.*, **112**, 2281-2292.

Philip, J., 1957: Evaporation, and moisture and heat fields in the soil. *J. Meteor*., **14**, 354-366.

Pielke, R. A., Sr., 2001: Influence of the spatial distribution of vegetation and soils on the preduction of cumulus convective rainfall. *Rev. Geophys.*, **39-2**, 151-177.

Reichle, R. H., D. B. McLaughlin, and D. Entekhabi, 2002a: Hydrologic data assimilation with an ensemble Kalman filter. *Mon. Wea. Rev*., **130**, 103-114.

----------, J. P. Walker, R. D. Koster, and P. R. Houser, 2002b: Extended versus ensemble Kalman filtering for land data assimilation. *J. Hydromet*., **3**, 728-740.

Rogers, E., D. Deaven and G. J. DiMego, 1995: The regional analysis system for the operational "early" Eta model: original 80-km configuration and recent changes. *Wea. Forecasting***, 10**, 810-825**.**

Rogers, E., T. L. Black, D. G. Deaven, G. J. DiMego, Q. Zhao, M. Baldwin, N. W. Junker and Y. Lin, 1996: Changes to the operational ``Early'' Eta analysis/forecast system at the National Centers for Environmental Prediction. *Wea. Forecasting*, **11** 391-413.

Sasamori, T., 1970: A numerical study of atmospheric and soil boundary layers. *J. Atmos. Sci.*, **27**, 1122-1137.

Segal, M., and R. W. Arritt, 1992: Nonclassical mesoscale circulations caused by surface sensible heat flux gradients. *Bull. Amer. Meteor. Soc*., **73**, 1593-1604.

Sellers, P. J., Y. Mintz, Y. C. Sud, and A. Dalcher, 1986: A simple biosphere model (SIB) for use with general circulation models. *J. Atmos. Sci*., **43**, 505-531.

Skamarock, W. C., J. B. Klemp, and J. Dudhia, 2001: Prototypes for the WRF (Weather Research and Forecasting) model. *Preprints, Ninth Conf. on Mesoscale Processes*, Fort Lauderdale, FL, Amer. Meteor. Soc., J11–J15.

Stensrud, D. J., J.-W. Bao, and T. T. Warner, 2000: Using initial conditions and model physics perturbations in short-range ensemble simulations of mesoscale convective systems. *Mon. Wea. Rev*., **128**, 2077-2107.

----------, and S. J. Weiss, 2002: Mesoscale model ensemble forecasts of the 3 May 1999 tornado outbreak. *Wea. Forecasting*, **17**, 526-543.

Szunyogh, I., and Z. Toth, 2002: The effect of increased horizontal resolution on the NCEP global ensemble mean forecasts. *Mon. Wea. Rev*., **130**, 1125–1143.

Tribbia, J. J., and D. P. Baumhefner, 2004: Scale interactions and atmospheric predictability: an updated perspective. *Mon. Wea. Rev*., **132**, 703-713.

Trier, S. B., F. Chen, and K. W. Manning, 2004: A study of convection initiation in a mesoscale model using high-resolution land surface initial conditions. *Mon. Wea. Rev.*, **132**, 2954-2976.

Wang, W., and N. L. Seaman, 1997: A comparison study of convective parameterization schemes in a mesoscale model. *Mon. Wea. Rev*., **125**, 252-278.

Wang, X., and C. H. Bishop, 2003: A comparison of breeding and ensemble transform Kalman filter ensemble forecast schemes. *J. Atmos. Sci*., **60**, 1140-1158.

Wicker, L. J., and W. C. Skamarock, 2002: Time splitting methods for elastic models using forward time schemes. *Mon. Wea. Rev*., **130**, 2088-2097

Xue, Y., P. J. Sellers, J. L. Kinter III, and J. Shukla, 1991: A simplified biosphere model for global climate studies. *J. Climate*, **4**, 345-364.

Yan, H., and R. A. Anthes, 1988: The effect of variations in surface moisture on mesoscale circulations. *Mon. Wea. Rev*., **116**, 192-208.

Zhang, D., and R. A. Anthes, 1982: A high-resolution model of the planetary boundary layer – sensitivity tests and comparison with SESAME-79 data. *J. Appl. Meteor*. **21**, 1594-1609.

List of Figure Captions

Figure 1: Outer and inner domains used in WRF experiment. Outer domain, common to all cases, is ~20 km grid spacing, and interior domains ~ 5 km. Domain (a) was used for the 12 July 2001 case, (b) for the 24 July 2002 case.

Figure 2: Data for 24-h simulation initialized on 1200 UTC 12 July 2001. (a) Analyzed mean sea-level pressure and 500 hPa geopotential height, (b) analyzed 24-h rainfall in subsequent 24 h, (c) NOAH analyzed soil moisture, (d) difference between NOAH and MOSAIC analyzed soil moisture in the top soil layer. Subsequent panels denote the forecast data from the 5-km simulations. (e) Accumulated 24-h forecast precipitation from NOAH5, (f) 24-h accumulated difference in precipitation between MOSAIC5 and NOAH5 simulations, (g) 12-h forecast 2-m temperature from NOAH5 simulation, and (h) 12-h forecast 2-m temperature difference between MOSAIC5 and NOAH5 simulations.

Figure 3: 3-hourly accumulated precipitation (panels a,d,g, and j) from NOAH5 simulation for 12 July 2001 case. 3-hourly accumulated precipitation differences between MOSAIC5 and NOAH5 simulations (panels b, e, h, and k). 3-hourly accumulated precipitation differences between scaled MOSAIC5 and NOAH5 simulations (panels c, f, i, and l), where the MOSAIC5 initial soil moisture has been replaced by an initial soil moisture that consists of the NOAH5 initial soil moisture plus 10 percent of the difference between MOSAIC5 and NOAH5 initial soil moistures.

Figure 4: (a) 24-h forecast accumulated precipitation from NOAH20KF simulation for 12 July 2001 case. (b) Difference in 24-h accumulated precipitation between MOSAIC20KF and NOAH20KF simulations. (c) 12-h forecast of 2-m temperature from NOAH20KF simulation, and (d) Difference in 12-h forecast of 2-m temperature between MOSAIC20KF and NOAH20KF simulations.

Figure 5: (a) 24-h forecast accumulated precipitation from NOAH20BMJ simulation for 12 July 2001 case. (b) Difference in 24-h accumulated precipitation between NOAH20BMJ and NOAH20KF simulations. (c) Difference in 12-h forecast of 2-m temperature between NOAH20BMJ and NOAH20KF simulations.

Figure 6: As in Figure 2, but for 24 July 2002.

Figure 7: As in Figure 4, but for 24 July 2002.

Figure 8: As in Figure 5, but 24 July 2002.

Figure 9: Box and whiskers plot of differences in (a) precipitation and (b) temperature forecasts induced by changing soil moisture at 5 or 20 km grid spacing, or the 20-km convective parameterization. In panel (a), the box and whisker diagrams indicate the 1st and 99th percentiles of the differences (dots), the 5th and 95th percentiles (error bars), the 33rd and 67th percentiles (tops and bottoms of colored boxes), and the 50th percentile (black line in middle of colored box). For precipitation, the differences are stratified by

the 24-h precipitation amount of the control forecast (NOAH5 or NOAH20KF) in the inner domain. For temperature, the statistics are accumulated over all grid points in the inner domain. Data beyond plotting range: the 1st and 99th percentiles for the precipitation difference of MOSAIC5 – NOAH5 when the control is > 40 mm is -97.1 and 84.7; for NOAH20BMJ – NOAH20KF is -91.9 and 82.0. For temperature, 1st percentile of the MOSAIC20KF – NOAH20KF is -15.8 C.

Figure 10: Frequency of 24-h precipitation amounts in inner domain for NOAH5, NOAH20KF, and NOAH20BMJ forecasts.

List of Table Captions

Table 1: List of names of experiments performed, as well as the associated soil moisture analysis used for initialization and the resolution and type of convective parameterization.

Experiment Name	Soil Analysis	Resolution	Convective Parameterization
NOAH5	NOAH	5 km	explicit
MOSAIC5	MOSAIC	5 km	explicit
NOAH20KF	NOAH	20 km	Kain-Fritsch
MOSAIC20KF	MOSAIC	20 km	Kain-Fritsch
NOAH20BMJ	NOAH	20 km	Betts-Miller-Janjic

Table 1: List of names of experiments performed, as well as the associated soil moisture analysis used for initialization and the resolution and type of convective parameterization.

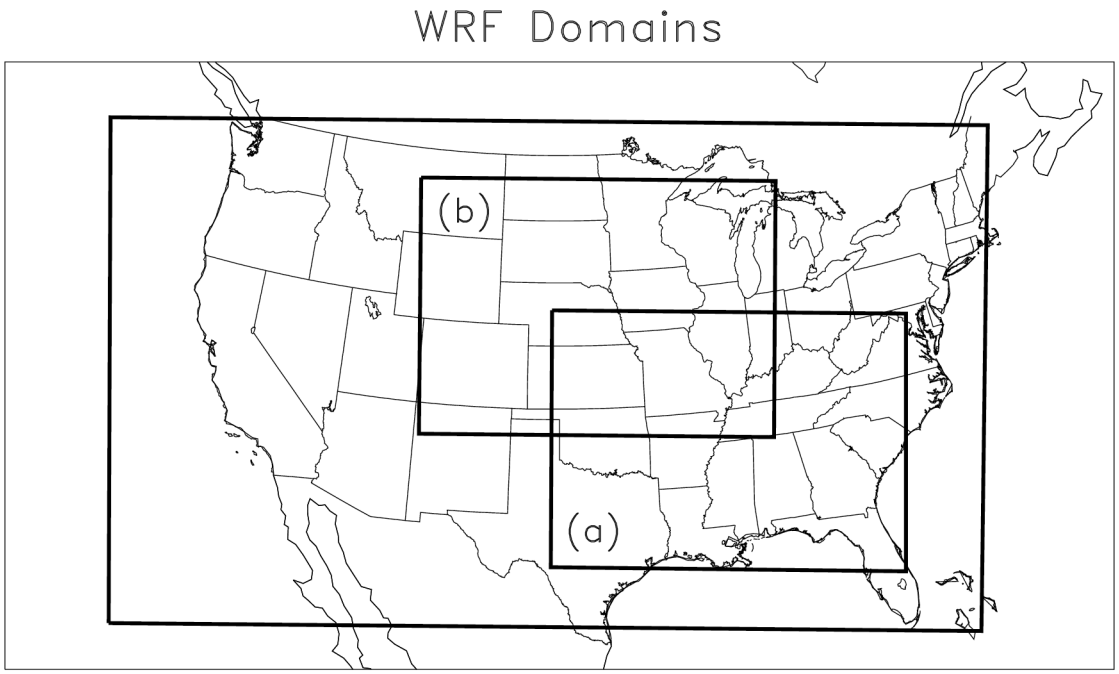

Figure 1: Outer and inner domains used in WRF experiment. Outer domain, common to all cases, is ~20 km grid spacing, and interior domains ~ 5 km. Domain (a) was used for the 12 July 2001 case, (b) for the 24 July 2002 case.

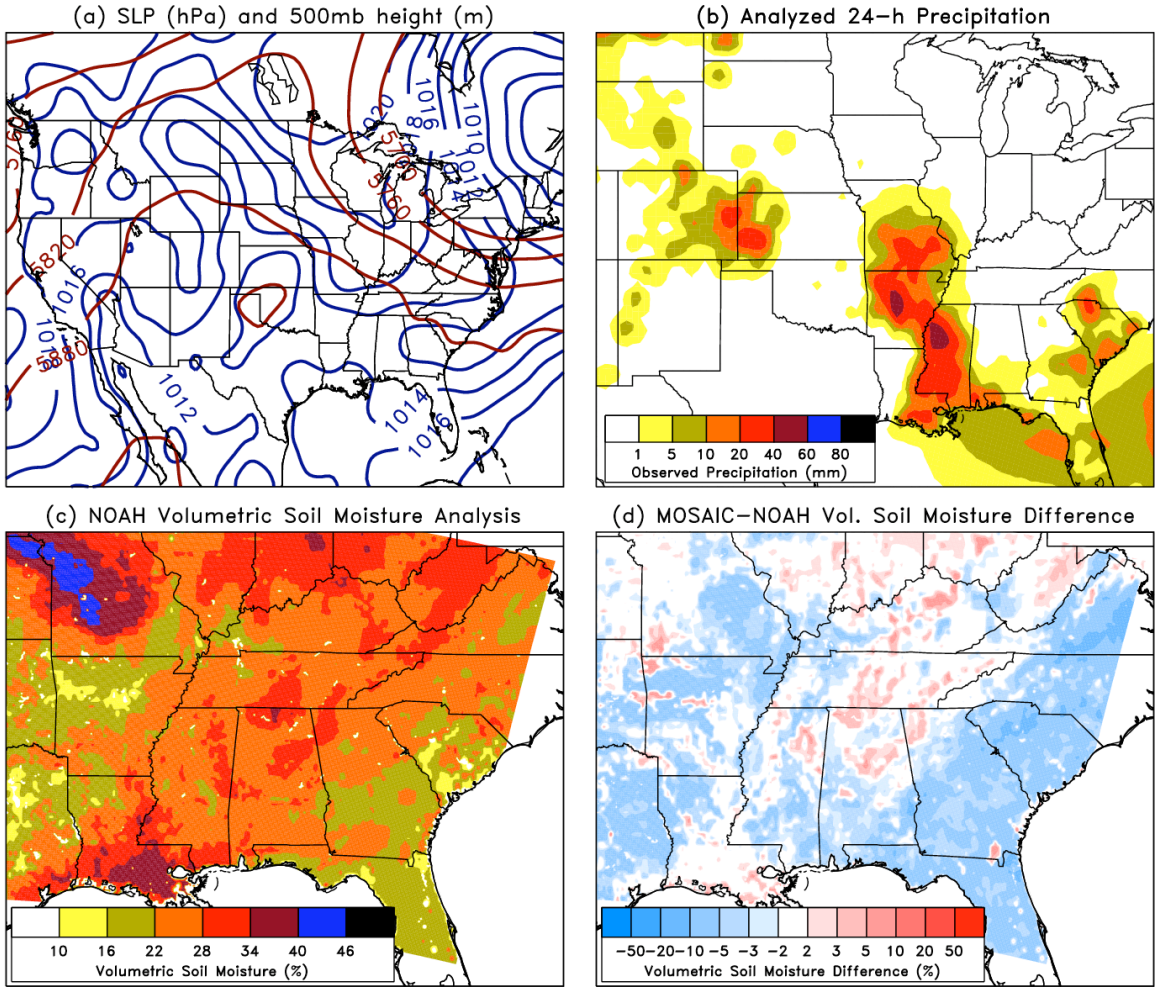

Figure 2: (see caption on next page)

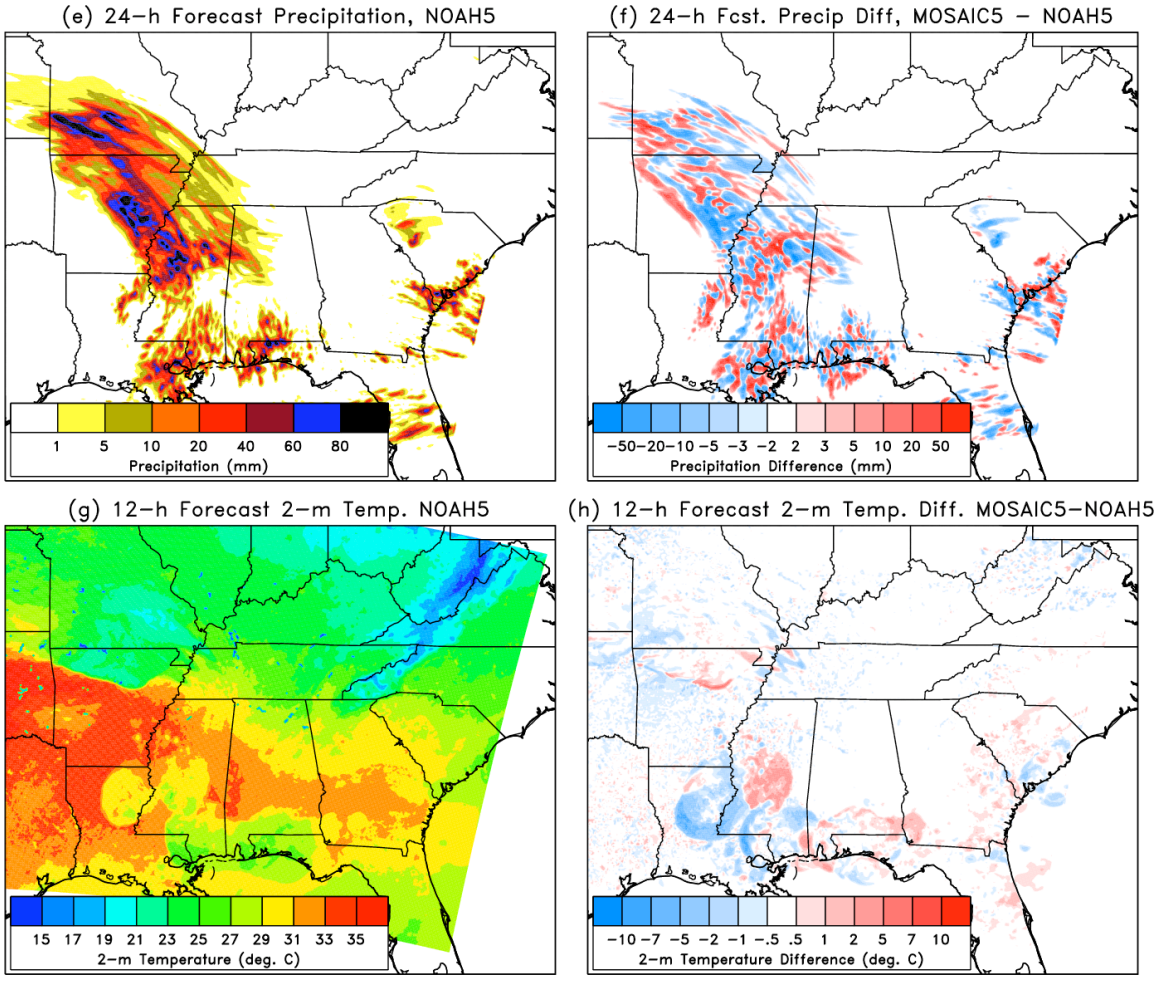

Figure 2: Data for 24-h simulation initialized on 1200 UTC 12 July 2001. (a) Analyzed mean sea-level pressure and 500 hPa geopotential height, (b) analyzed 24-h rainfall in subsequent 24 h, (c) NOAH analyzed soil moisture, (d) difference between NOAH and MOSAIC analyzed soil moisture in the top soil layer. Subsequent panels denote the forecast data from the 5-km simulations. (e) Accumulated 24-h forecast precipitation from NOAH5, (f) 24-h accumulated difference in precipitation between MOSAIC5 and NOAH5 simulations, (g) 12-h forecast 2-m temperature from NOAH5 simulation, and (h) 12-h forecast 2-m temperature difference between MOSAIC5 and NOAH5 simulations.

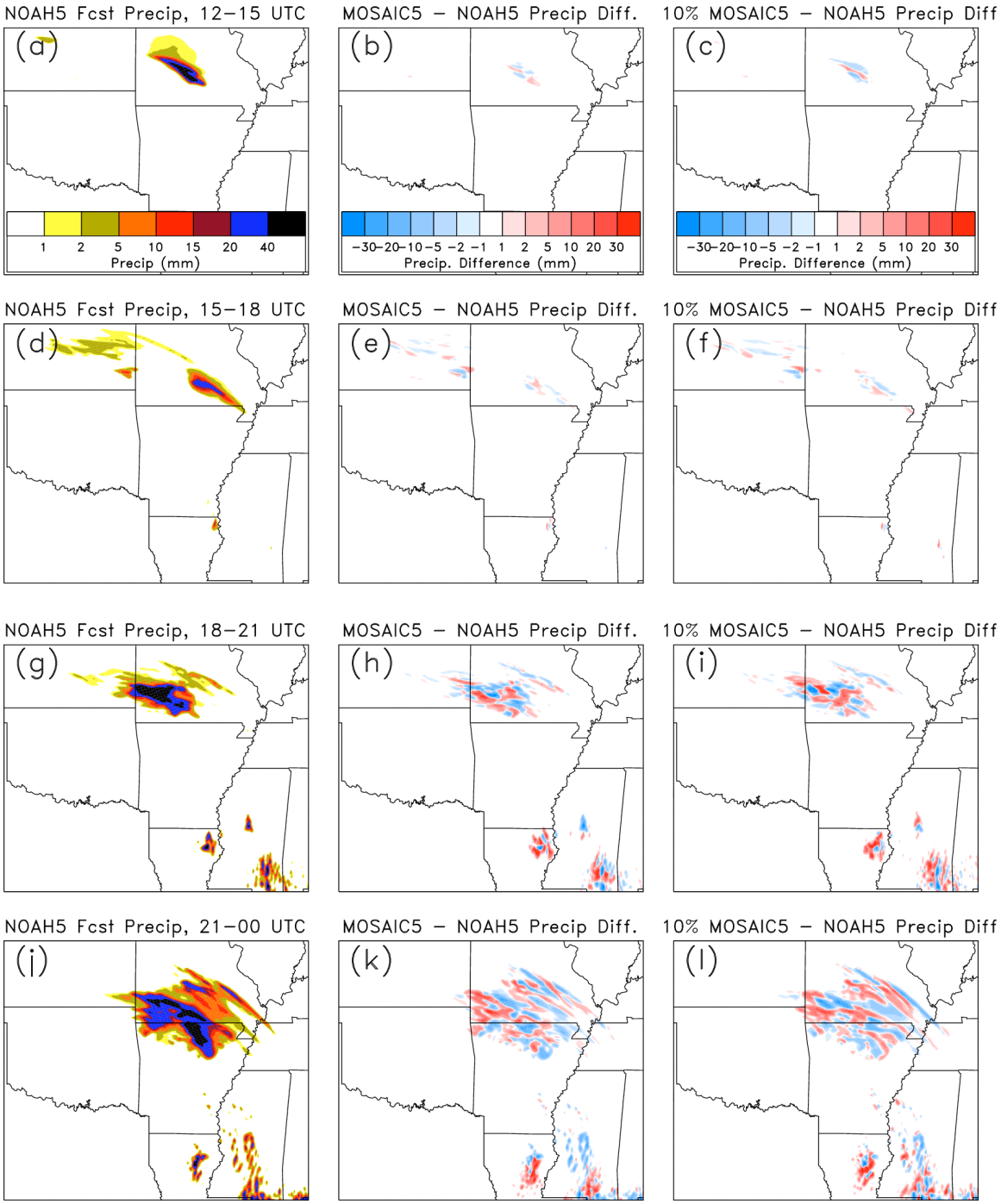

Figure 3: 3-hourly accumulated precipitation (panels a,d,g, and j) from NOAH5 simulation for 12 July 2001 case. 3-hourly accumulated precipitation differences between MOSAIC5 and NOAH5 simulations (panels b, e, h, and k). 3-hourly accumulated precipitation differences between scaled MOSAIC5 and NOAH5 simulations (panels c, f, i, and l), where the MOSAIC5 initial soil moisture has been replaced by an initial soil moisture that consists of the NOAH5 initial soil moisture plus 10 percent of the difference between MOSAIC5 and NOAH5 initial soil moistures.

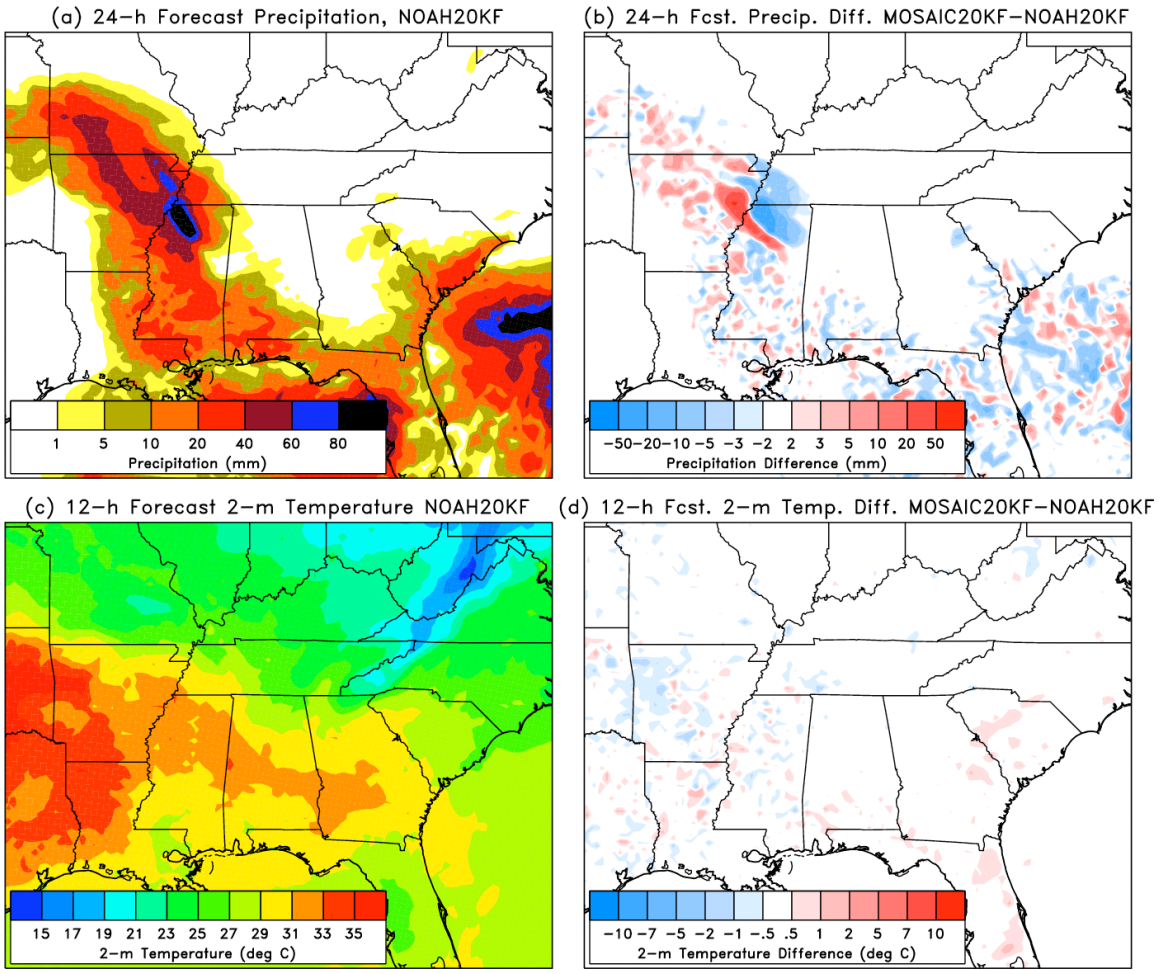

Figure 4: (a) 24-h forecast accumulated precipitation from NOAH20KF simulation for 12 July 2001 case. (b) Difference in 24-h accumulated precipitation between MOSAIC20KF and NOAH20KF simulations. (c) 12-h forecast of 2-m temperature from NOAH20KF simulation, and (d) Difference in 12-h forecast of 2-m temperature between MOSAIC20KF and NOAH20KF simulations.

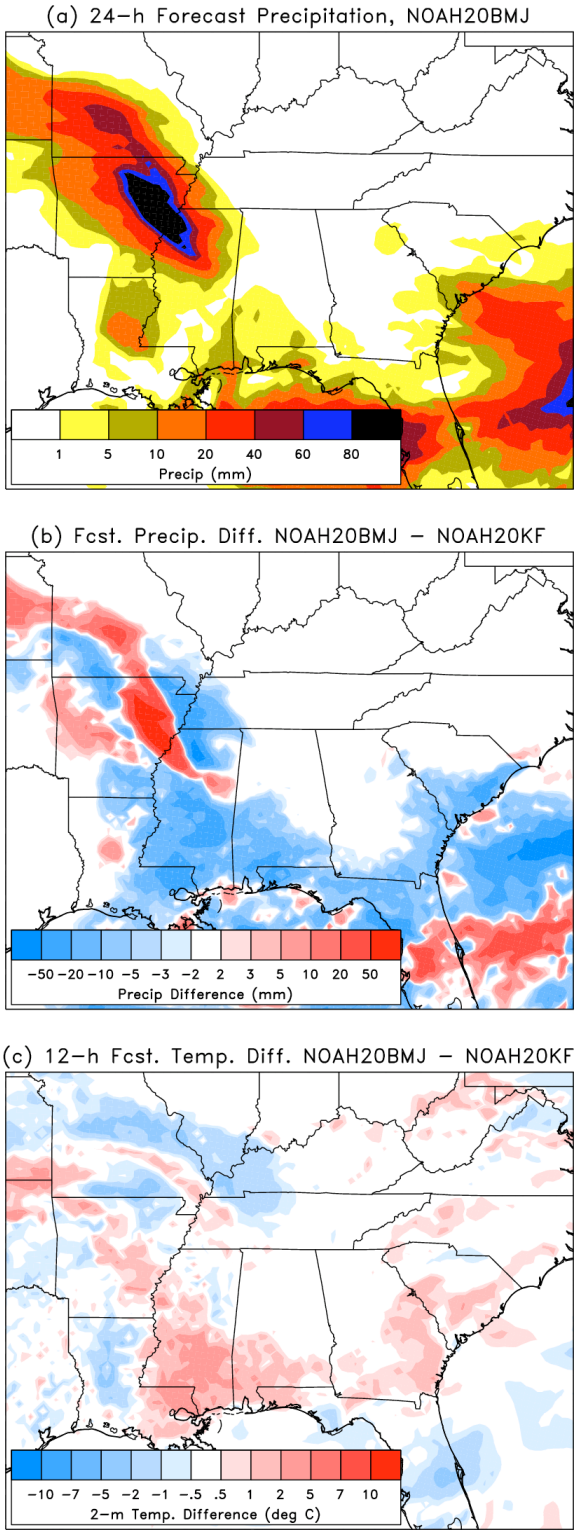

Figure 5: (a) 24-h forecast accumulated precipitation from NOAH20BMJ simulation for 12 July 2001 case. (b) Difference in 24-h accumulated precipitation between NOAH20BMJ and NOAH20KF simulations. (c) Difference in 12-h forecast of 2-m temperature between NOAH20BMJ and NOAH20KF simulations.

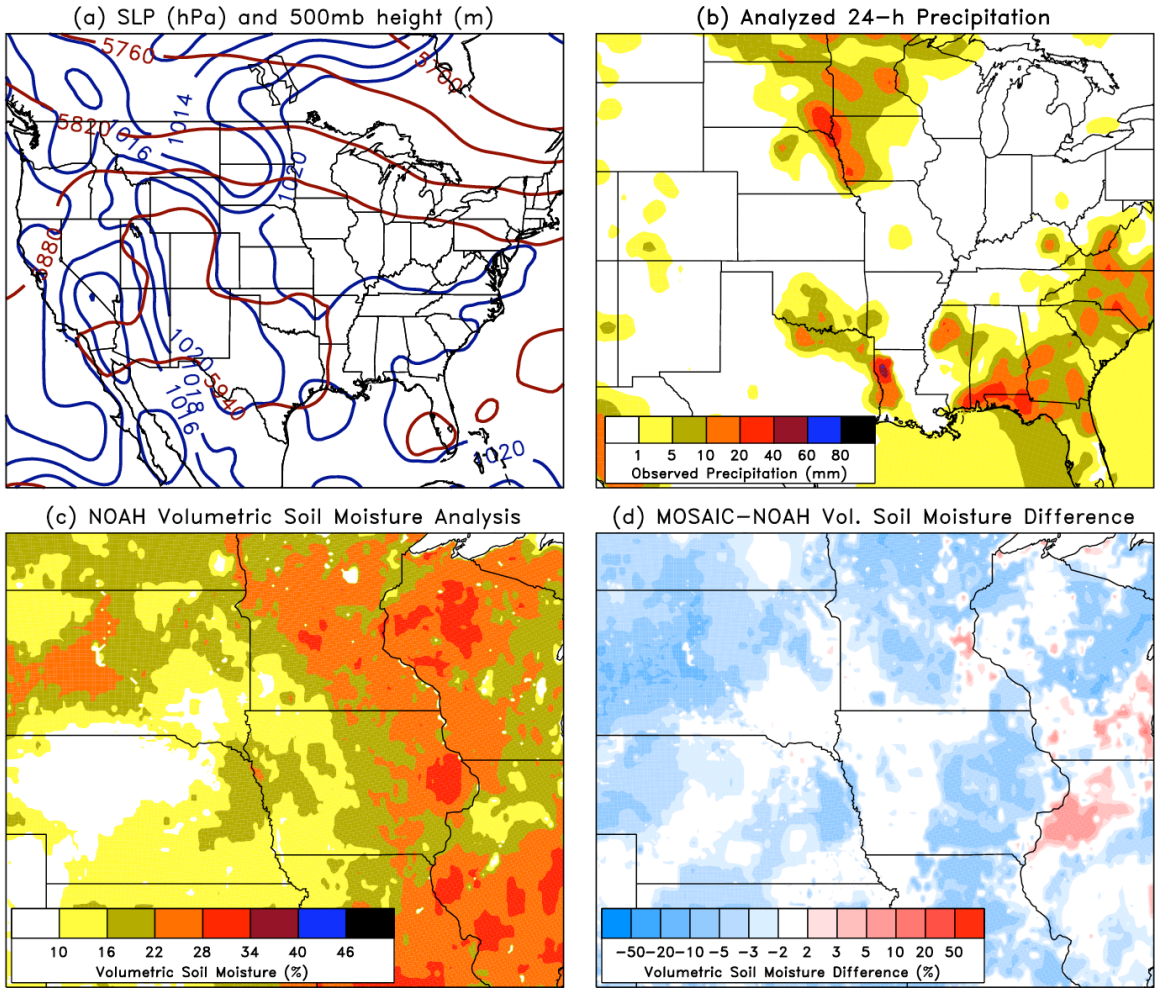

Figure 6 : (see caption on next page).

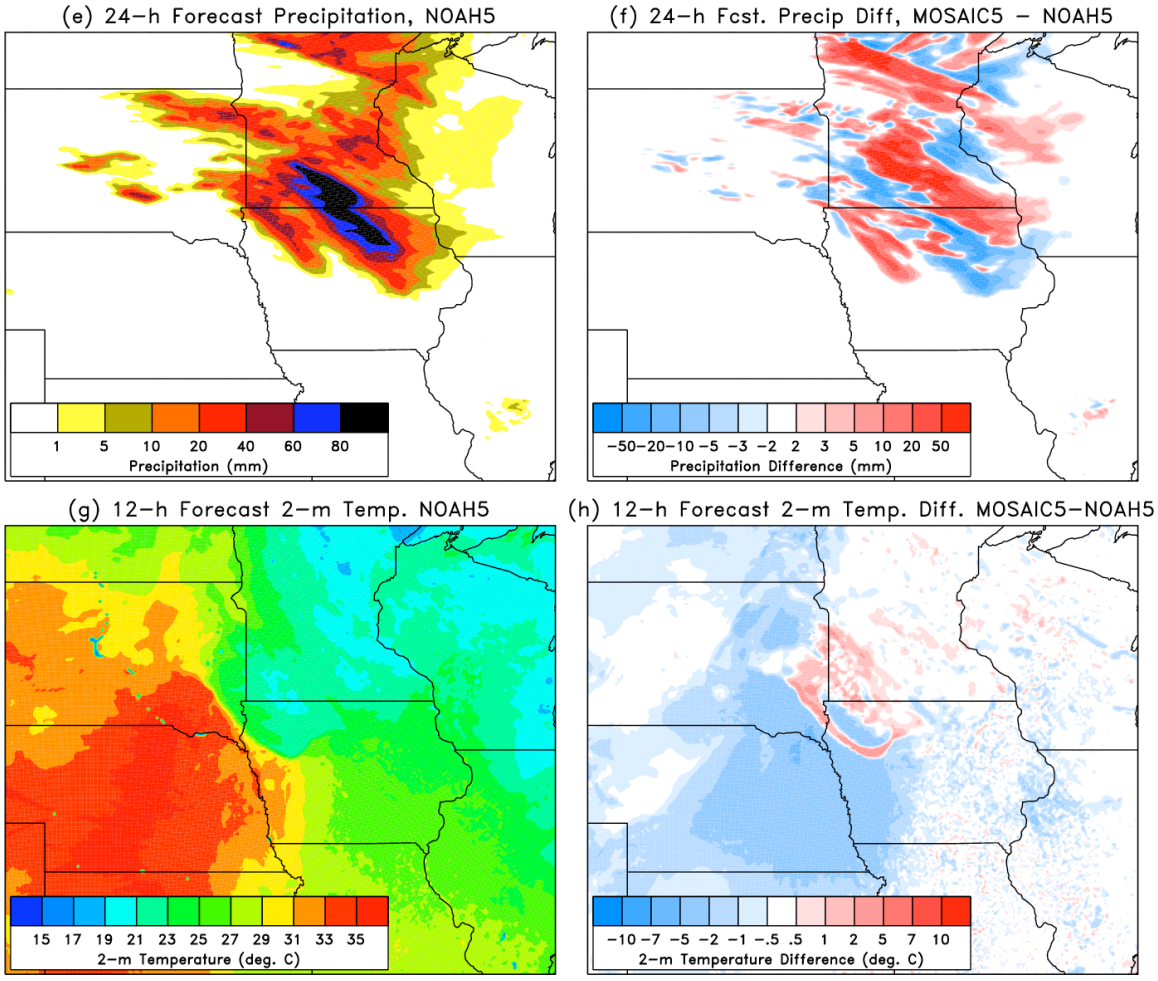

Figure 6: As in Figure 2, but for 24 July 2002.

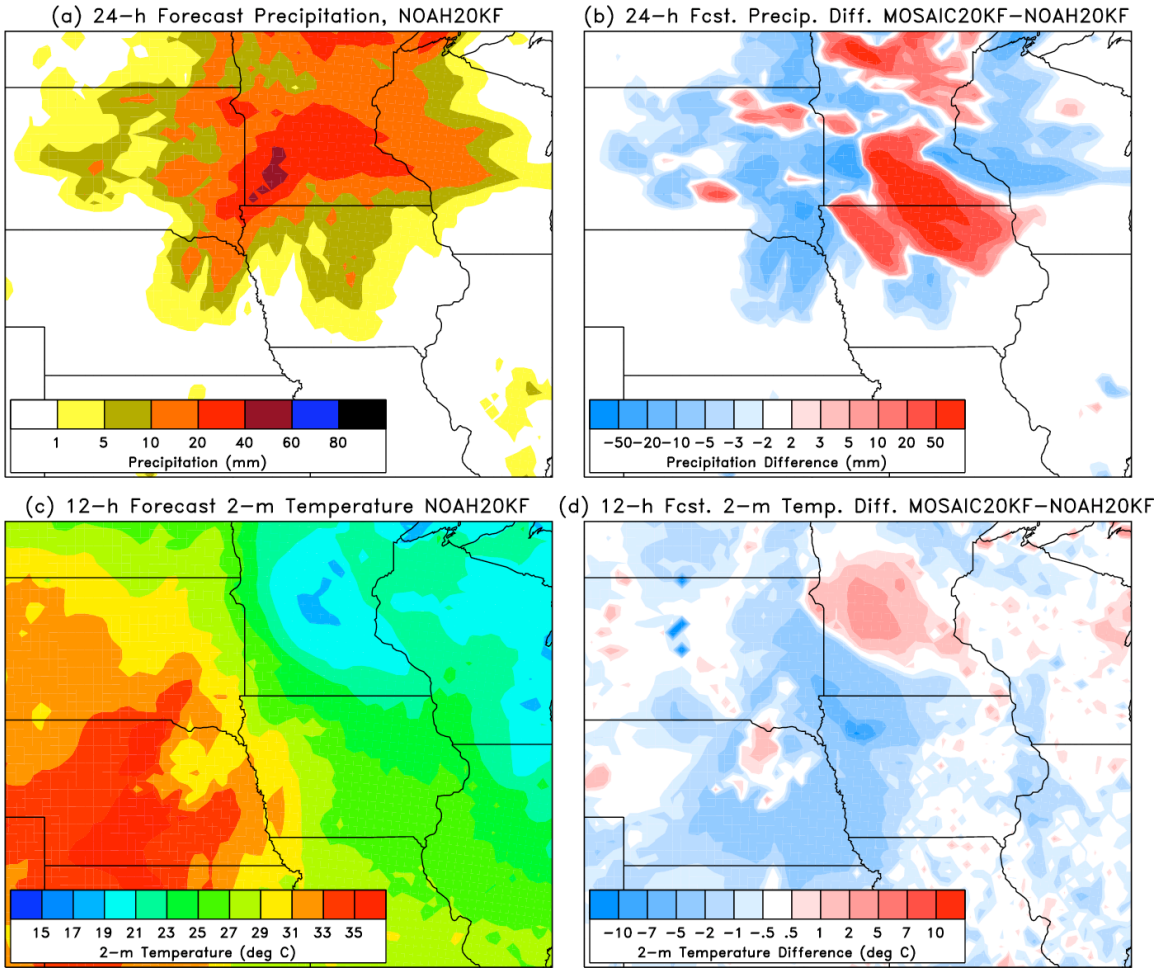

Figure 7: As in Figure 4, but for 24 July 2002.

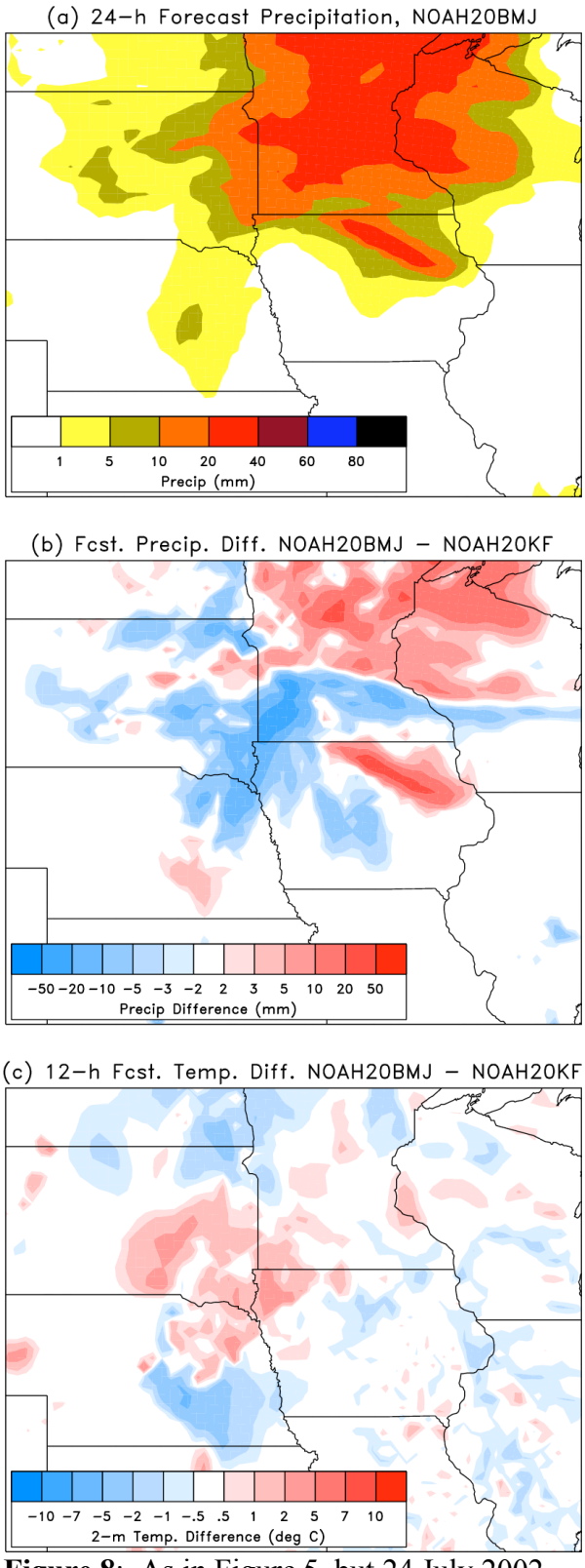

Figure 8: As in Figure 5, but 24 July 2002.

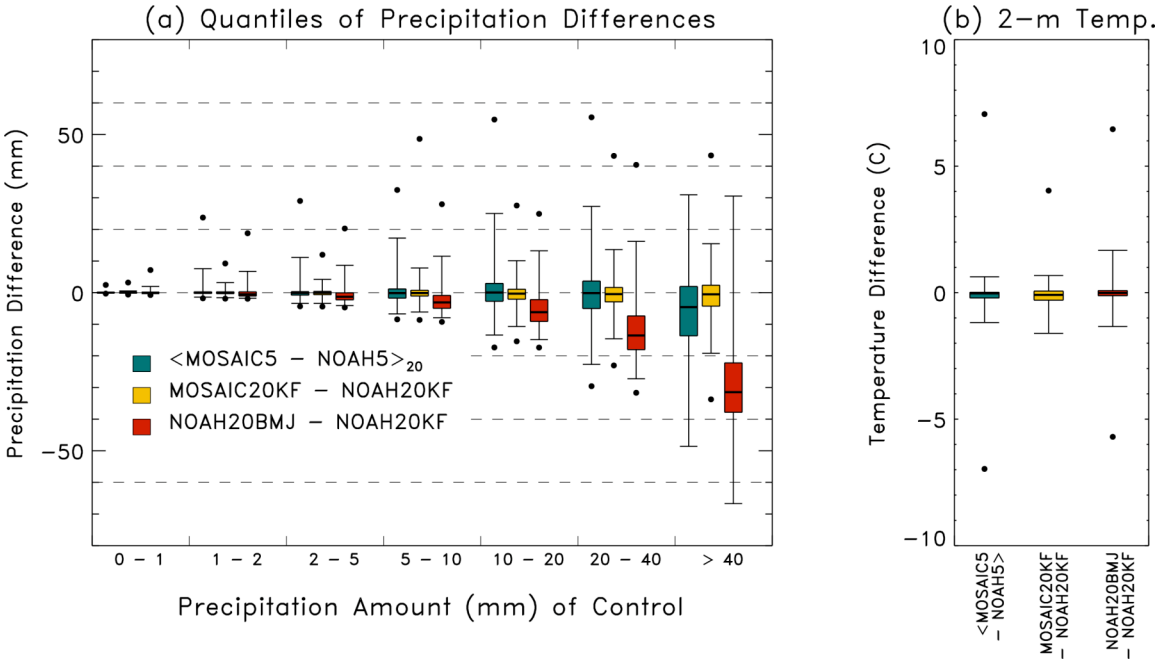

Figure 9: Box and whiskers plot of differences in (a) precipitation and (b) temperature forecasts induced by changing soil moisture at 5 or 20 km grid spacing, or the 20-km convective parameterization. In panel (a), the box and whisker diagrams indicate the 1st and 99th percentiles of the differences (dots), the 5th and 95th percentiles (error bars), the 33rd and 67th percentiles (tops and bottoms of colored boxes), and the 50th percentile (black line in middle of colored box). For precipitation, the differences are stratified by the 24-h precipitation amount of the control forecast (NOAH5 or NOAH20KF) in the inner domain. For temperature, the statistics are accumulated over all grid points in the inner domain. Data beyond plotting range: the 1st and 99th percentiles for the precipitation difference of MOSAIC5 – NOAH5 when the control is > 40 mm is -97.1 and 84.7; for NOAH20BMJ – NOAH20KF is -91.9 and 82.0. For temperature, 1st percentile of the MOSAIC20KF – NOAH20KF is -15.8 C.

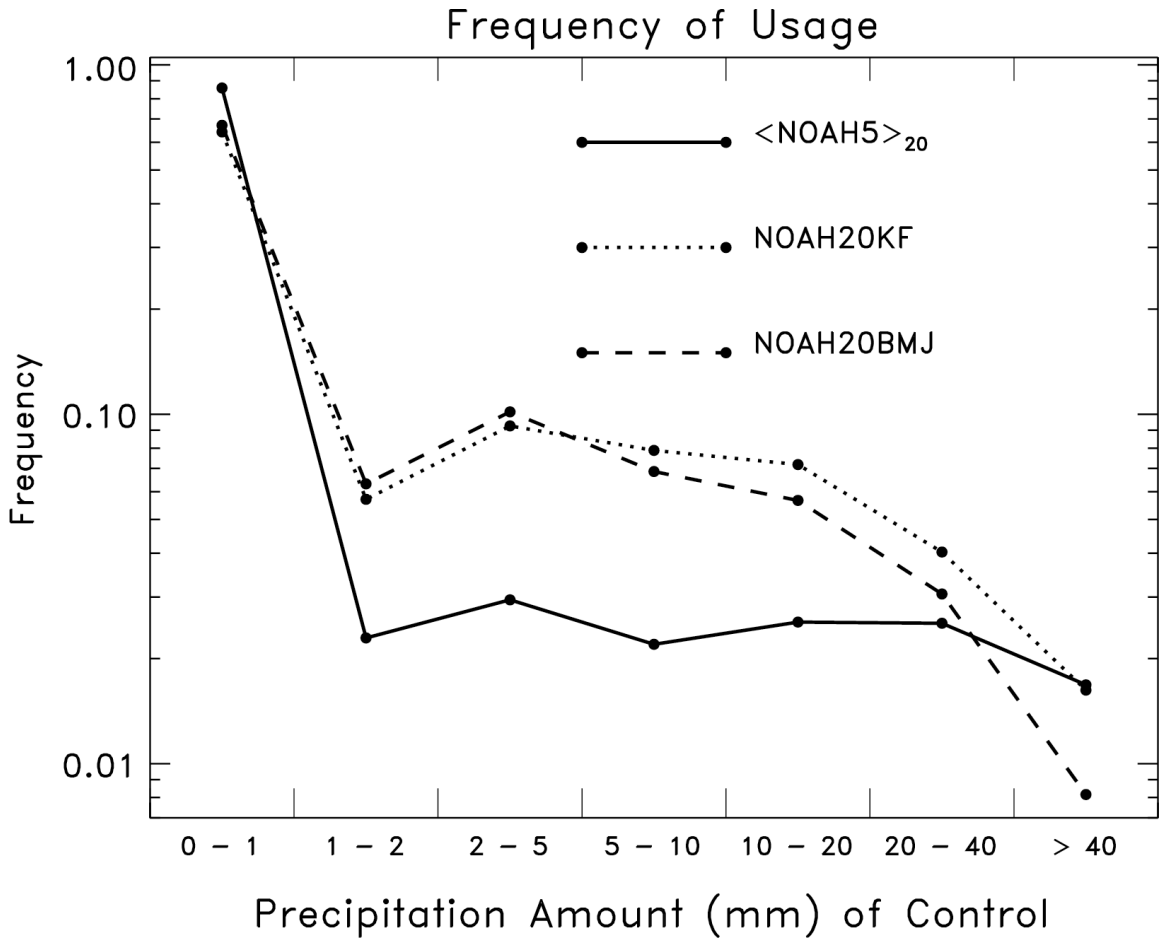

Figure 10: Frequency of 24-h precipitation amounts in inner domain for NOAH5, NOAH20KF, and NOAH20BMJ forecasts.